Journal of Neurochemistry

JOURNAL OF NEUROCHEMISTRY | 2008 | 107 | 1709–1721 doi: 10.1111/j.1471-4159.2008.05737.x

Secretory vesicle rebound hyperacidification and increased quantal size resulting from prolonged methamphetamine exposure

Dmitriy Markov,*[,1,2] Eugene V. Mosharov,*[,2] Wanda Setlik,† Michael D. Gershon† and David Sulzer*[,‡,§]

*Department of Neurology, Columbia University, College of Physicians and Surgeons, New York, NY, USA
†Department of Anatomy and Cell Biology, Columbia University, College of Physicians and Surgeons, New York, NY, USA
‡Departments of Psychiatry and Pharmacology, Columbia University, College of Physicians and Surgeons, New York, NY, USA
§Division of Molecular Therapeutics, New York State Psychiatric Institute, New York, NY, USA

Abstract

Acute exposure to amphetamines (AMPHs) collapses secretory vesicle pH gradients, which increases cytosolic catecholamine levels while decreasing the quantal size of catecholamine release during fusion events. AMPH and methamphetamine (METH), however, are retained in tissues over long durations. We used optical and electron microscopic probes to measure the effects of long-term METH exposure on secretory vesicle pH, and amperometry and intracellular patch electrochemistry to observe the effects on neurosecretion and cytosolic catecholamines in cultured rat chromaffin cells. In contrast to acute METH effects, exposure to the drug for 6–48 h at 10 μM and higher concentrations produced a concentration-dependent rebound hyperacidification of secretory vesicles. At 5–10 μM levels, prolonged METH increased the quantal size and reinstated exocytotic catecholamine release, although very high (> 100 μM) levels of the drug, while continuing to produce rebound hyperacidification, did not increase quantal size. Secretory vesicle rebound hyperacidification was temperature dependent with optimal response at ~37°C, was not blocked by the transcription inhibitor, puromycin, and appears to be a general compensatory response to prolonged exposure with membranophilic weak bases, including AMPHs, methylphenidate, cocaine, and ammonia. Thus, under some conditions of prolonged exposure, AMPHs and other weak bases can enhance, rather than deplete, the vesicular release of catecholamines via a compensatory response resulting in vesicle acidification.

Keywords: amperometry, chromaffin cells, cytosolic catecholamine, LysoSensor Yellow/Blue DND-160, methamphetamine, vesicular pH.

J. Neurochem. (2008) **107**, 1709–1721.

Amphetamine (AMPH) and methamphetamine (METH) have been prescribed to over 19 million Americans (NSDUH 2003 report) for the treatment of attention deficit hyperactivity disorder (ADHD) and other affective conditions, and are illicitly self-administered by over 25 million people worldwide (United Nations Office on Drugs and Crime 2007 report), either at very high doses by chronic drug abusers (Gettig *et al.* 2006), or at lower doses to alleviate fatigue and promote wakefulness. In abuse and some therapeutic settings, AMPHs are consumed several times a day and are eliminated quite slowly with a half-life of 10–24 h (see Materials and methods). Few studies, however, have examined the long-term effects of AMPHs on neurosecretion.

Acute exposure to AMPHs rapidly collapses the acidic pH gradient in secretory vesicles, redistributes stored

Received July 2, 2008; revised manuscript received September 25, 2008; accepted October 9, 2008.

Address correspondence and reprint requests to David Sulzer, Department of Neurology, Columbia University, 650 West 168th Street, Black Building Room 309, New York, NY 10032, USA.
E-mail: ds43@columbia.edu
[1]The present address of Dmitriy Markov is the Department of Cell Biology, UMDNJ-SOM, Stratford, New Jersey 08084, USA.
[2]These authors contributed equally to this study.

Abbreviations used: ADHD, attention deficit hyperactivity disorder; AMPH, amphetamine; AO, acridine orange; CV, cyclic voltammetry; DAMP, 3-(2,4 dinitroanilino)-3′-amino-*N*-methyl dipropylamine; IPE, intracellular patch electrochemistry; LDCV, large dense core vesicle; LSYB, LysoSensor Yellow/Blue DND-160; MDC, monodancylcadaverine; METH, methamphetamine; PBS, phosphate-buffered saline; RT, room temperature.

transmitter from vesicles to the cytosol, and decreases the quantal size of stimulation-dependent exocytosis (Johnson 1988; Sulzer and Rayport 1990; Sulzer *et al.* 1992; Jones *et al.* 1998; Mundorf *et al.* 1999; Mosharov *et al.* 2003). Additionally, AMPHs release catecholamines in a stimulation-independent manner by inducing reverse transport from the cytosol to the extracellular milieu via actions on plasma membrane uptake transporters (Fischer and Cho 1979; Sulzer *et al.* 1995; Sonders *et al.* 1997; Jones *et al.* 1998; Kahlig *et al.* 2005). Together with additional properties of these drugs, including an inhibition of dopamine catabolism and an activation of its synthesis (Sulzer *et al.* 2005), the net effect of acute METH or AMPH is to reduce stimulation-evoked catecholaminergic neurotransmission and induce stimulation-independent, non-exocytotic transmitter release.

Here, we compare the impact of acute and prolonged METH exposure on evoked adrenaline release by examining secretory vesicle pH, cytosolic catecholamine levels, and quantal secretory vesicle transmission in adrenal chromaffin cells. We show that, in contrast to acute METH effects that inhibit evoked catecholamine secretion, long-term drug treatment elicits a delayed reacidification of secretory vesicles, resulting in *increased* quantal size at pharmacologically relevant METH concentrations. The data thus indicate that prolonged AMPH exposure promotes an adaptation that we term *rebound hyperacidification* which reverses the decrease in quantal size, and augments rather than inhibits stimulation-dependent secretory catecholaminergic transmission.

Materials and methods

Chemicals and cell culture

Chemicals were purchased from Sigma-Aldrich (St. Louis, MO, USA) unless otherwise stated. Animal protocols were approved by the Columbia University Institutional Animal Care and Use Committees. Rat-derived postnatal chromaffin cells were isolated and cultured in a 5% CO_2 incubator at 37°C as previously described (Mosharov *et al.* 2003). All experiments were conducted between days 3 and 4 post-plating. Stock solutions of METH (100 mM) and other weak bases were added directly to the culture medium for the time indicated and washed out immediately prior to the measurements. For electron microscopy, the dishes were prepared with Aclar coverslips but were otherwise treated identically.

Amperometric recordings

Solutions used for amperometric recordings were as follows. The bath saline (pH 7.4) contained (in mM) 128 NaCl, 2 KCl, 1 NaH_2PO_4, 2 $MgCl_2$, 1.2 $CaCl_2$, 10 glucose, and 10 HEPES–KOH. Secretagogue solution was the same except 90 NaCl and 40 KCl. Secretagogue was applied by local perfusion through a pressurized glass micropipette (Picospritzer; General Valve Co., Fairfield, NJ, USA) for 5 s at ~10 μm from the cell. A 5 μm diameter carbon fiber electrode held at +700 mV was pressed against the cell surface and catecholamine oxidation was monitored as amperometric current spikes. The current was filtered using a 4-pole 5 kHz Bessel filter built into an Axopatch 200B amplifier (Axon Instruments, Foster City, CA, USA) and sampled at 25 kHz (ITC-18; Instrutech, Great Neck, NY, USA). After secretagogue application, the amperometric current was recorded for 60 s and the data were analyzed using a locally written routine (see Mosharov and Sulzer 2005 for details) in IGOR Pro (WaveMetrics, Lake Oswego, OR, USA). The current was digitally filtered using a low-pass binomial 600 Hz filter and the root mean square of the noise on the first derivative of the current (dI/dt) was measured in a segment of the trace that did not contain spikes; dI/dt was then used to detect amperometric events that were 4.5-fold larger than the root mean square of the noise. To improve the quality of spike detection, the current was additionally filtered using low-pass binomial 150 Hz filter before taking dI/dt (Mosharov and Sulzer 2005). For each amperometric spike, the following shape characteristics were determined: quantal size (Q, pC), spike amplitude (I_{max}, pA), duration at half-height ($t_{½}$, ms), rise-time between 25% and 75% of I_{max} excluding the pre-spike foot (t_{rise}, ms), and the incline of the rising phase (slope, pA/ms). The falling phase of a spike was characterized by two time constants (τ_1 and τ_2, ms) of the double-exponential fit of the current between 25% of I_{max} and spike's end. The number of catecholamine molecules released from individual vesicles (Q_N) was calculated as $Q_N = Q/(n \cdot F)$, where F = 96 485 C/mole is Faraday's constant and $n = 2$ is the number of electrons donated by each catecholamine molecule (Bruns and Jahn 1995). Spikes with I_{max} smaller than 3 pA and traces with fewer than 10 amperometric spikes were excluded from the analysis.

Intracellular patch electrochemistry (IPE)

Measurements of cytosolic catecholamine concentrations were performed as previously described (Mosharov *et al.* 2003). Briefly, the concentration of cytosolic catecholamine was determined using a cyclic voltammetric (CV) mode of electrochemical detection; 300 mV/ms ramps of voltage were applied over 100 ms intervals to the carbon fiber electrode positioned inside the patch pipette. After achieving the whole cell configuration, cytosolic catecholamines were monitored as an oxidation wave and their concentration was calculated using the calibration curves. The initial cytosolic catecholamine concentration was estimated using images of the cell and the patch pipette to account for molecule dilution within the pipette tip.

When a carbon fiber electrode is employed in CV mode of detection, a unique red-ox profile (voltammogram) provides a means to distinguish catechols from other oxidazable cytosolic metabolites. The electrode in CV mode is 15- to 20-fold more sensitive to catecholamines (dopamine, norepinephrine, and epinephrine) than to other catechol species present within the cytosol, thus allowing one to discriminate against the presence of 3,4-dihydroxy-L-phenylalanine (L-DOPA), 3,4-dihydroxyphenylacetic acid (DOPAC), and 3,4-Dihydroxyphenyl ethylene glycol (DOPEG) (Mosharov *et al.* 2003).

Measurements of secretory vesicle acidity using acridine orange

At each time point of incubation with METH, chromaffin cells were rinsed once with drug-free Dulbecco's phosphate-buffered saline (PBS), pH 7.4, and treated with 10 nM acridine orange (AO) for 10 minutes at 37°C. Cultures were rinsed with 3 mL PBS twice and series of images were taken from randomly chosen cells over the following 5 minutes using 480 nm excitation and 535 nm emission

filter set for FITC/AO (Chroma Technology Co., Rockingham, VT, USA). Images were acquired with a cooled charge-coupled device Star I camera (Photometrics, Tuscon, AZ, USA) operated by IPLAB software v. 3.1.1 (BD Biosciences Bioimaging, Rockville, MD, USA). The pixel intensities of all images were normalized in 8-bit (byte) monochrome image range (0–255). The pixel intensity value was averaged from the total cell area excluding the nucleus using 'Segmentation' and 'Quantify Segments' modes in IPLAB software. Average pixel intensity of the background staining was quantified from the cell-free area of the image and subtracted from the average value of cell-specific AO staining. For each time point, the intensity of AO staining is shown as the average of the mean ± SEM from at least 30 individual cells.

Ratiometric pH measurements with LysoSensor Yellow/Blue DND-160 *in situ*

Cells were incubated with 5 μM LysoSensor Yellow/Blue DND-160 (LSYB; Invitrogen Co., Carlsbad, CA, USA) in CO_2-conditioned culture medium for 5 minutes at 37°C, washed with dye-free PBS, and imaged on inverted fluorescent microscope using 40× Plan-Neofluar oil objective (Carl Zeiss MicroImaging Inc., Thornwood, NY, USA) and two customized filter sets. Both filter sets shared the same 365 nm excitation filter that corresponded to the isobestic point of LSYB excitation spectrum. The emission filters were 445 nm (blue) and 510 nm (yellow), corresponding to the maxima of pH-sensitive peaks of LSYB emission spectrum (Diwu *et al.* 1999). Images were acquired using Star I camera operated by IPLAB software within 10 min following LSYB addition. Following background subtraction and accounting for bleaching, the mean pixel values from the cell body excluding the nucleus were calculated as described above for AO. Yellow to blue ratio of fluorescence intensities was further used to calculate vesicular pH employing the exponential fit parameters from the calibration curve. To calibrate LSYB emission ratios for a range of pH values *in situ*, vesicles were saturated with LSYB as described, and then the extracellular media for LSYB-filled cells was replaced with a buffer of known pH in the presence of monensin, a Na^+/H^+ antiporter, and nigericin, a K^+/H^+ antiporter, which act to bring the cytosol and chromaffin vesicles to the pH of the surrounding media (Holopainen *et al.* 2001). Cells were incubated with 5 μM LSYB in CO_2-conditioned culture medium for 20 min at 37°C and washed with dye-free PBS at room temperature (RT). Next, the saline was exchanged to a buffer of known pH (values from 3.5 to 6.5), 10 μM monensin and 10 μM nigericin were applied, and images were acquired within the following 15 min and processed as above (Fig. S1). Although the leakage of the dye from vesicles to the cytosol cannot be avoided during the calibration procedure, this was unlikely to affect the resulting LSYB calibration curve, because the pH in the vesicles and the cytosol was equilibrated to that of the extracellular buffer. Yellow/blue values from triplicate groups of 10–20 individual cells were averaged and used to build the calibration curve. Ratios ≥ 3 SD from the mean were excluded from analysis. To follow the rapid changes in vesicular pH induced by an exposure to weak bases, the cells were pre-incubated with 5 μM LSYB for 5 min, the dye was washed out with PBS, and immediately after the addition of a weak base, yellow and blue images were acquired from 10 randomly chosen cells. The ratios from 10 dishes were averaged and pH values calculated from the calibration curve as described.

Two-photon images of LSYB-stained chromaffin cells were acquired on DM6000B microscope (Leica Microsystems Inc., Bannockburn, IL, USA) equipped with a 63 × 0.9 water immersion objective. Excitation wavelength was at 750 nm and two emission channels had bandwidths of 400–450 nm and 520–600 nm.

Staining with monodancylcadaverine

Cells were labeled with monodancylcadaverine (MDC) as described (Larsen *et al.* 2002). Briefly, cells were incubated with 50 μM MDC in CO_2–conditioned culture medium for 20 minutes at 37°C. After extensive wash with drug-free conditioned media, cells were incubated in CO_2 incubator for 10 minutes, washed twice with PBS and imaged on inverted fluorescent microscope using 40× Plan-Neofluar oil objective. Live cell images were taken with a customized filter set with 335 nm excitation and 525 nm emission filters (Chroma Technology Co.). Pixel intensity values were compared as described for AO.

Immunogold electron microscopy of DAMP in chromaffin vesicles

3-(2,4 Dinitroanilino)-3′-amino-*N*-methyl dipropylamine (DAMP) is a weak base that is trapped in acidic compartments and can be detected in tissues with antibodies to dinitrophenol (Anderson *et al.* 1984). DAMP immunoreactivity was detected in chromaffin cells as previously described (Pothos *et al.* 2002). Briefly, the cultures were treated with 100 μM METH from 1 or 24 h before adding 50 μM DAMP (Molecular Probes, Eugene, OR, USA) for 30 min. Following a 5 min rinse in PBS, cells were fixed with 4% *p*-formaldehyde, 0.1% glutaraldehyde, and 3% sucrose in 0.1 M phosphate buffer, pH 7.4 for 1 h at 25°C. The fixed cells were washed twice for 5 min in PBS and mordanted with 0.25% tannic acid in 100 mM sodium phosphate buffer containing 3.5% sucrose for 1 h at 4°C. Specimens were then quenched with 50 mM NH_4Cl, washed with 100 mM sodium maleate containing 4% sucrose, pH 6.2, and stained *en bloc* with maleate-buffered 2% uranyl acetate. The stained cells were dehydrated to 70% ethanol at 4°C; the temperature was then lowered to −20°C for dehydration to 90% ethanol, clearing and embedding in LR Gold Resin (London Resin Co., Reading, UK). The LR Gold was polymerized with ultraviolet light at −20°C. Thin sections were picked up on Ni grids that had previously been layered with Formvar (Electron Microscopy Sciences, Hatfield, PA, USA). The sections on the grids were blocked with 10% donkey serum with Tris-buffered saline containing Tween 20 (10 mM Tris, pH 7.2, 500 mM NaCl, and 0.05% Tween 20) for 30 min at 20°C. Sections were incubated overnight with rabbit polyclonal antibodies to dinitrophenol (1 : 200; Sigma-Aldrich). Grids were subsequently washed in blocking solution and incubated for 2 h at 25°C with donkey anti-rabbit antibodies coupled to 18 nm particles of colloidal gold (1 : 40; Jackson ImmunoResearch, West Grove, PA, USA). The sections were washed in PBS, post-fixed with 2.5% glutaraldehyde, and stained with aqueous 2% osmium, uranyl acetate, and lead citrate. Sections were examined with a 1200 EX electron microscope (JEOL Ltd., Tokyo, Japan).

Estimation of vesicular pH gradients in DAMP-containing organelles

The internal pH of cellular organelles at the ultrastructural level was measured by determining the partition of DAMP, as previously

published (Anderson *et al.* 1984; Orci *et al.* 1994). For each micrograph, the density of immunogold particles was measured in an area outside the cell ($D_{extracell}$), the nucleus ($D_{nucleus}$), a lysosome ($D_{lysosome}$), and in 20 randomly chosen large dense core vesicles (LDCVs) ($D_{vesicle}$ = total area/total number of gold particles). Intravesicular and lysosomal pHs were then estimated as:

$$pH = 7.0 - \log\left(\frac{D_{vesicle\ or\ lysosome} - D_{extracell}}{D_{nucleus} - D_{extracell}}\right)$$

and expressed as an average of the mean pH values from 10 to 15 cells in each group. Alternatively, intravesicular pH of individual vesicles was calculated using the same formula and distributions of vesicle pH for each group were plotted as cumulative histograms in Excel (Microsoft, Redmond, WA, USA).

Estimation of pharmacologically relevant METH concentration

Methamphetamines and AMPH are not discriminated by humans, are similarly retained in tissues, and have nearly identical mechanisms of action and abilities to induce catecholamine release (Sulzer *et al.* 2005). These drugs are self-administered in typical doses of 250–500 mg by occasional users and at higher doses by chronic abusers (personal communication, Perry N. Halkitis, New York University). There is little data on the kinetics of METH and AMPH retention in the body after such large doses, but case reports showed plasma drugs concentrations of 30–100 μM and higher (Cravey and Baselt 1968; Orrenius and Maehly 1970; Jones and Holmgren 2005) (see also (Talloczy *et al.* 2008) for the discussion of relevant plasma levels in drug addicts). Studies on the pharmacokinetics of METH levels in healthy adult human volunteers show that following a single oral 10–30 mg dose (0.14–0.43 mg/kg), plasma METH concentration reaches 0.1–0.7 μM; AMPHs are eliminated quite slowly by excretion and cytochrome P450 metabolism with the half-life of ~12 h (Perez-Reyes *et al.* 1991; Cook *et al.* 1992; Cho *et al.* 2001; Harris *et al.* 2003; Schepers *et al.* 2003; Kim *et al.* 2004). Because METH doses administered to patients with ADHD are typically higher (5–40 mg single doses; 0.17–1.33 mg/kg), and because AMPHs are retained in the brain and kidneys at > 10-fold higher levels than in the plasma (Melega *et al.* 1995; Riviere *et al.* 2000), 5–10 μM METH concentrations and incubation times used in our experiments were assumed to be close to those in the brain following clinical administration.

Relationship between quantal size and vesicle pH

Catecholamine gradients across the secretory vesicles membrane depends on the electrochemical proton gradient:

$$\mathrm{Log}\left(\frac{[CA]_{vesicle}}{[CA]_{cytosol}}\right) = \frac{\Delta\Psi \cdot F}{R \cdot T} + 2 \cdot \Delta pH,$$

where $[CA]_{vesicle}$ and $[CA]_{cytosol}$ are catecholamine concentrations inside and outside the vesicle, $\Delta\Psi$ is electrical gradient, F is Faraday's constant, R is the universal gas constant, T is the absolute temperature, and ΔpH is the difference in pH between the vesicle and the cytosol. Assuming that electric gradient and pH in the cytosol are constant, a linear correlation is expected between $[CA]_{vesicle}$ and $[CA]_{cytosol}$, and between $[CA]_{vesicle}$ and the square of the proton concentration in the vesicle, $[H^+]_{vesicle}$:

$$[CA]_{vesicle} = A \cdot [CA]_{cytosol} \cdot [H^+]^2_{vesicle},\ \text{where}\ A = 10^{\frac{\Delta\Psi \cdot F}{R \cdot T}} / [H^+]^2_{cytosol}$$

Statistical analysis

Unless stated otherwise, data were analyzed by one-way ANOVA followed by Tukey's *post hoc* test. For the normal probability plots the data are presented as Log(Q_N), the distribution of which is close to normal (Finnegan *et al.* 1996). Occasional large events with log quantal sizes > 3 SD greater than the geometric mean of Log(Q_N) were excluded from the analysis. Data on all graphs are presented as mean ± SEM.

Results

Prolonged METH causes rebound hyperacidification of chromaffin granules *in situ*

To investigate the effect of METH treatment on secretory vesicle acidity, we labeled LDCV in METH-treated chromaffin cells with AO, a fluorescent vital dye that has been used to study the acidification of secretory organelles, including synaptic vesicles (Tabb *et al.* 1992) and adrenal chromaffin granules (Steyer *et al.* 1997; Pothos *et al.* 2002).

As previously reported (Sulzer and Rayport 1990), acute (1 h) exposure of cultured chromaffin cells to METH resulted in a concentration-dependent decrease in vesicle-associated AO fluorescence, indicating a collapse of the vesicular proton gradient (data not shown). In contrast, we observed a gradual increase in AO fluorescence after prolonged exposure to METH, suggesting that chromaffin vesicles in drug-treated cells became more acidic than those in untreated cells (Fig. 1), a response we label *rebound hyperacidification*. The effect was reversible because 3–6 h after washout of METH (Fig. 1, white arrow) vesicular pH returned to initial levels. Remarkably, chromaffin granules in

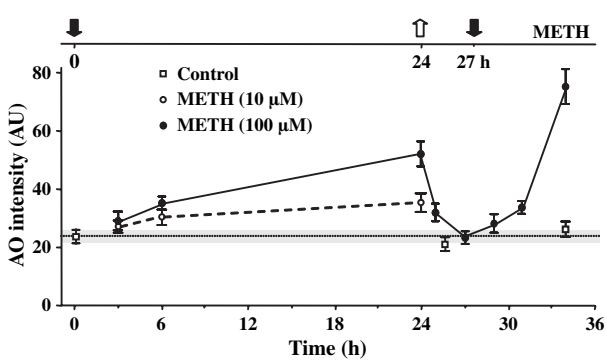

Fig. 1 Time course of METH-induced vesicle acidification. Time course of vesicle pH changes assessed by the retention of AO in cells treated with 10 μM and 100 μM METH. The upper bar shows the time scale of two consecutive METH additions (solid arrows) and a drug washout (open arrow). AO was added for 10 min before each measurement. Data points represent mean fluorescence intensities ± SEM from n = 30–40 cells. Dotted line and shadowed box represent the mean ± SEM in control cells at time zero.

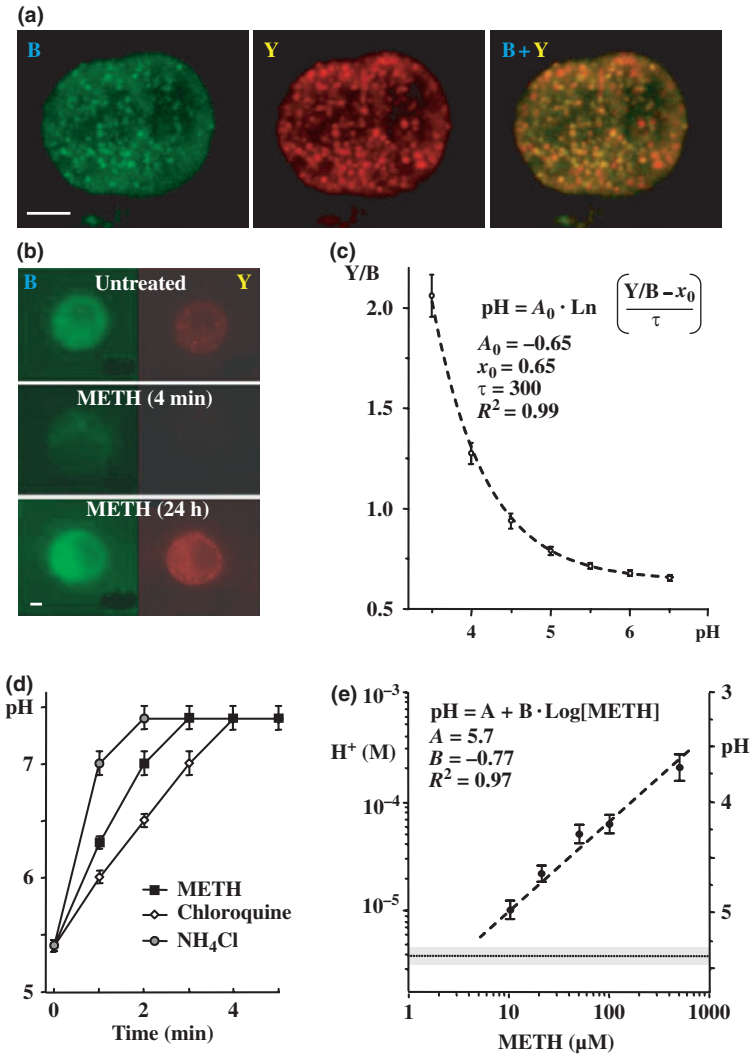

Fig. 2 *In situ* measurement of vesicular pH in chromaffin secretory vesicles using LSYB. (a) Maximal projection two-photon images of LSYB-stained chromaffin cells. Two emission channels 445 nm (blue) and 510 nm (yellow) were pseudo-colored as green and red, correspondingly. Note the punctate LSYB staining with negligible signal from the cytosol. Scale bar, 10 μm. (b) Examples of LSYB epifluorescence images taken at 510 nm (Y) and 445 nm (B) from untreated cells and cells exposed to 100 μM METH for 4 min or 24 h; λ_{ex} = 365 nm. Scale bar, 10 μm. (c) Calibration curve for ratiometric measurement of vesicular pH. (d) Time course of vesicular pH changes in chromaffin cells acutely treated with 100 μM METH, 100 μM chloroquine and 10 mM ammonium chloride. n = 10 cells at each experimental group. (e) Vesicular proton concentration and pH in cells treated with different METH concentrations for 24 h. All treatment groups were significantly different from untreated cells (p < 0.005 by one-way ANOVA). Dotted line and shadowed box represent the mean ± SEM in untreated cells.

cells exposed to the second METH dose after drug washout acidified more rapidly then during the first exposure. Thus, the cellular response that produced rebound hyperacidification, once induced, remained active even after METH removal.

To study the changes in vesicle acidity in more detail, we employed LSYB, a fluorescent pH probe that provides quantitative measurements of vesicular acidity. LSYB has two pH-sensitive fluorescence emission peaks and the ratio of the fluorescence intensities at their maxima can be calibrated to determine pH within acidic organelles in living cells (Diwu *et al.* 1999). As was seen with AO, LSYB rapidly accumulated in chromaffin cells with punctate distribution that filled almost the entire cytosol, consistent with the distribution of the secretory vesicles (Fig. 2a and b). We found that LSYB could be used to estimate intravesicular pH in a range of <3.5 to ~6 (Figs 2c and S1), as was reported earlier (Holopainen *et al.* 2001).

Intravesicular pH in untreated chromaffin cells, determined from LSYB ratiometric measurements, was 5.4 ± 0.1, a value similar to estimates made by alternative methods, including electron spin resonance, uptake of radiolabeled tracers by isolated vesicles, and quantitative immunocytochemistry *in situ* (Pollard *et al.* 1979; Njus *et al.* 1986; Johnson 1988; Pothos *et al.* 2002). METH exposure alkalinized the vesicles within minutes, as did ammonium chloride and chloroquine, two other broadly used amphiphilic weak bases (Fig. 2b and d). As was seen with AO, vesicles accumulated more LSYB in their lumen after prolonged METH treatment and changes in Y/B ratio confirmed the enhanced vesicle acidity. The accumulation of LSYB was abolished by pre-treatment of cells with a monensin/nigericin cocktail (data not shown), indicating that changes in the fluorescence of the dye were indeed caused by a corresponding change in vesicular pH, rather than by an interaction between LSYB and METH. There was a linear relationship between the logarithm of the METH concentra-

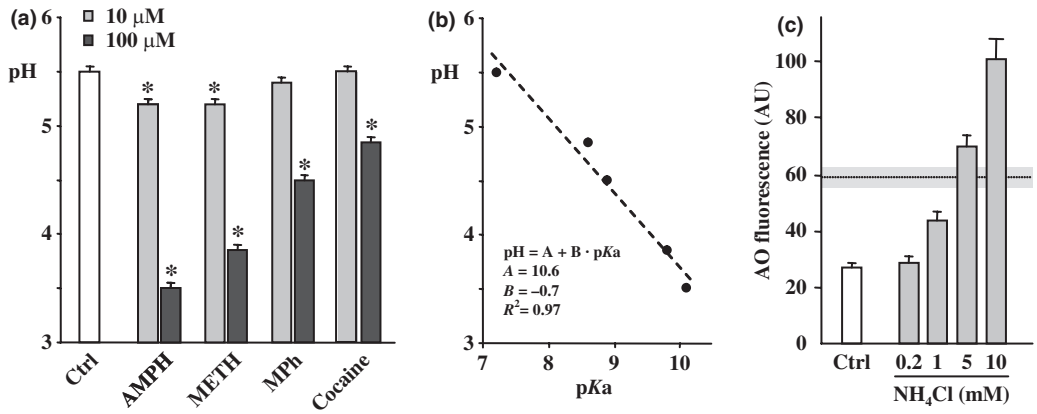

Fig. 3 Dependence of vesicle acidity on weak-base properties of various drugs. (a) Vesicle pH in chromaffin cells treated for 24 h with drugs at 10 μm (gray bars) and 100 μM (black bars) concentrations; $n = 30$ cells in each group, $^*p < 0.05$ compared with untreated cells. (b) Dependence of vesicular pH on pK_a values of the drugs. All weak bases were used at 100 μM concentrations for 24 h. Acidity of vesicles in cells treated with 50 μM puromycin (pK_a = 7.2) for 6 h is shown as the leftmost point. The values of pK_a for other drugs were from the online Hazardous Substances Data Bank (http://toxnet.nlm.nih.gov/): AMPH – 10.1, METH – 9.9, MPh – 8.8, cocaine – 8.6. (c) Dose-dependent accumulation of AO in vesicles of chromaffin cell treated with ammonium chloride for 24 h. Dotted line and shadowed box represent the mean ± SEM in cells treated with 100 μM METH for 24 h.

tion and intravesiclular pH, which reached apparent values lower than 4.0 following the highest doses of METH (Fig. 2e).

To investigate whether the effect of METH on organelle acidification was specific to the drug, we examined the internal pH of secretory vesicles in cells that were treated for 24 h with weak base psychostimulants other than METH. While AMPH was as potent as METH in inducing vesicle hyperacidification, identical concentrations of methylphenidate and cocaine were significantly less efficient than METH (Fig. 3a). The magnitude of drug-induced hyperacidification was related reciprocally to the pK_a of the psychostimulants examined (Fig. 3b), suggesting that the effect on intravesicular pH was dependent on the weak base properties of the drugs. However, ammonia, an inorganic weak base that, like METH, has a pK_a of 9.2 but is less efficient than METH at alkalinizing vesicles, was also relatively inefficient at producing rebound vesicle hyperacidification (Fig. 3c). This observation highlights the importance of other factors, including the abilities of various weak bases to cross plasma and vesicle membranes either resulting from the lipophilicity of the compounds or their facilitated diffusion/active transport.

Ultrastructural analysis of METH-treated chromaffin granules

The intracytoplasmic compartments responsible for the trapping of AO and LSYB cannot be identified with certainty by fluorescence microscopy. We therefore studied the partitioning of DAMP, another weak base, which also accumulates in acidic compartments, but can be fixed *in situ* and visualized by electron microscopic immunocytochemistry (Anderson *et al.* 1984; Pothos *et al.* 2002). Intracellular DAMP was detected immunocytochemically by post-embedding labeling with immunogold. The number of gold particles within an organelle reflects the intracellular concentration of DAMP, which is in turn proportional to the proton gradient across the membrane that separates the interior of the organelle from the cytosol. By quantifying the density of gold particles, therefore, the ΔH^+ could be estimated. The density of particles in nuclei was also determined and used as a reference to estimate the pH within other organelles, assuming that the intranuclear pH 7.0 was unaffected by the treatments. The density of gold particles in lysosomes served as a positive control. Lysosomes were defined as acidic, large, pleomorphic, perinuclear organelles, whereas secretory vesicles had a uniform shape, were <300 nm in diameter and contained a round dense core. The number of lysosomes was considerably smaller than the number of LDCVs (~1 to 50 in Controls).

As expected, DAMP accumulated in LDCVs in both untreated and METH-treated cells (Fig. 4a). The average vesicular and lysosomal pH in untreated cells was 5.7 ± 0.1 and 5.2 ± 0.1, respectively; acute exposure to METH (1 h, 100 μM) alkalinized both organelles to near neutral pHs (Fig. 4b and c). Confirming the data obtained with AO and LSYB, vesicles in cells treated with METH for 24 h trapped significantly more DAMP than vesicles of untreated cells, reaching a pH that was equivalent to that of lysosomes (pH 5.1 ± 0.1); this decrease in intravesicular pH represented a fourfold increase in the intravesicular proton concentration over that found in vesicles of untreated cells. Neither acute, nor prolonged METH exposure significantly altered the profile of individual secretory vesicles (mean area of

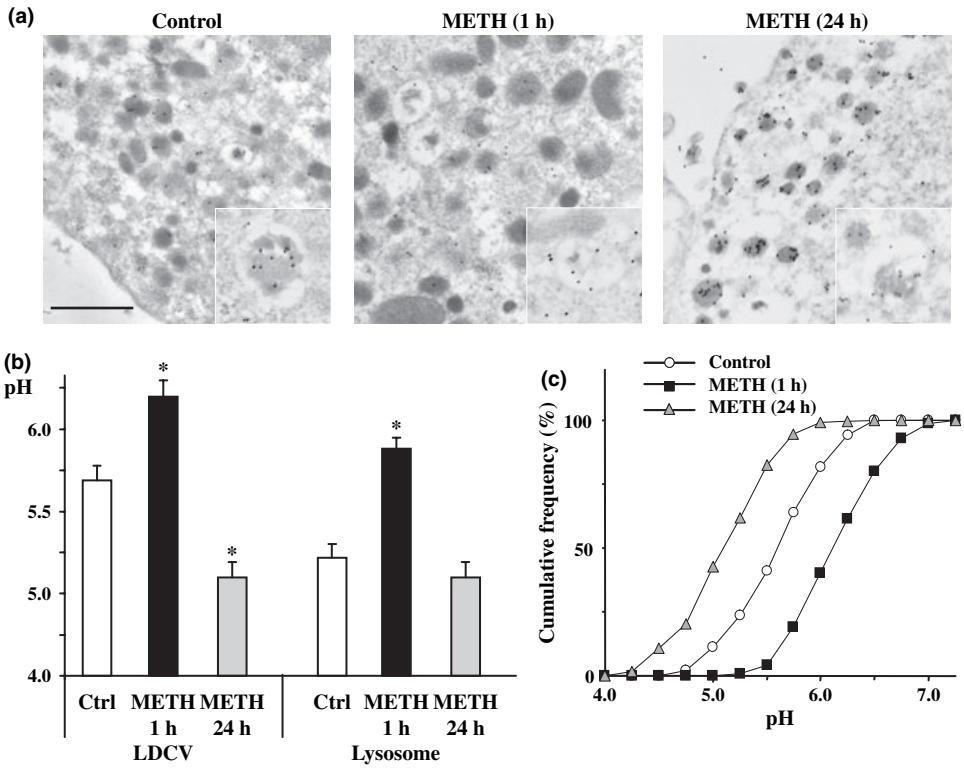

Fig. 4 Immunoelectron microscopy of chromaffin granules in METH-treated cells. (a) Representative micrographs of DAMP-stained untreated cells and cells treated with 100 μM METH for 1 h or 24 h. The scale bar, 500 nm. Insets show lysosomes at the same scale. (b) Quantification of vesicular and lysosomal pH (see Materials and methods); *$p < 0.05$ from untreated cells. (c) Cumulative distribution of pH values of individual secretory vesicles in untreated and METH-treated chromaffin cells ($n = 212$ vesicles in control, 146 in 1 h METH, and 224 in 24 h METH). All curves are different from each other with $p < 0.001$ by Kolmogorov–Smirnov test.

16 600 ± 1300 nm^2 in control vs. 15 400 ± 1600 nm^2 and 13 500 ± 1100 nm^2 in cells treated with 100 μM METH for 1 h or 24 h, correspondingly; mean ± SEM). While the degree of pH decrease estimated from DAMP partitioning was lower than that from LSYB measurements (see Discussion), the results confirm that long-term METH treatment induced rebound hyperacidification in secretory vesicles. The effect of prolonged METH treatment was specific for secretory vesicles, because lysosomes in cells treated with the drug for 24 h recovered their acidity to control levels, but did not hyperacidify (Fig. 4a and b).

To determine whether rebound hyperacidification resulted from changes in the expression levels of enzymes and transporters, we measured intravesicular pH in cells that were incubated with METH in the presence of puromycin to block protein translation (Fig. 5a). Puromycin treatment did not prevent vesicle hyperacidification, indicating that the phenomenon does not require *de novo* protein synthesis. To corroborate the involvement of an enzymatic component in the maintenance and alteration of vesicle acidity, we measured the temperature dependence of intravesicular pH in cultured chromaffin cells. The curve relating the dependence of pH to temperature, either in the presence or in the absence of METH, was saddle-shaped with the maximal proton gradient achieved at ~37°C (Fig. 5b). Such a relationship is common for mammalian enzymes, as increased enzymatic activity at higher temperatures is overcome by heat-induced protein denaturation and deactivation resulting from a cellular heat-shock response. However, when METH-specific rebound hyperacidification was displayed as the difference between intravesicular pH in untreated and drug-treated cells, the response increased steadily with temperature, reaching the highest difference at 42°C (Fig. 5c). We conclude that enzymatic processes involved in the induction of METH-related alterations in cellular homeostasis were not inactivated even at 42°C, similar to thermostable lysosomal enzymes (Keech and Wills 1979) or Na^+-K^+-ATPase (Burdon *et al.* 1984).

Changes in cytosolic and vesicular catecholamine concentrations after prolonged METH

To investigate whether METH-induced rebound hyperacidification affected the vesicular content of catecholamines, we used amperometric recordings with carbon fiber electrodes to determine the number of catecholamine molecules released per secretory vesicle during exocytosis. The relationship

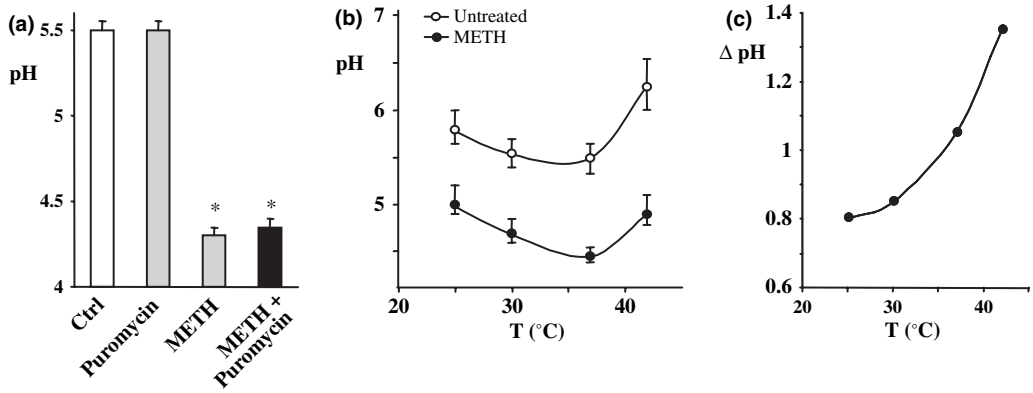

Fig. 5 Involvement of enzymatic component in METH-induced vesicle hyperacidification. (a) Effect of translation inhibitor, puromycin, on METH-induced hyperacidification of chromaffin secretory vesicles. Cells were treated with 100 μM METH for 6 h with or without 50 μM puromycin, followed by pH measurements with LSYB; n = 30–40 cells, $^*p < 0.005$ compared with untreated cells. (b) Temperature dependence of vesicle pH in control cells and those treated with 100 μM METH for 6 h; n = 40 cells in each group. (c) Temperature dependence of METH-induced vesicle hyperacidification calculated as the difference between the two curves on (b).

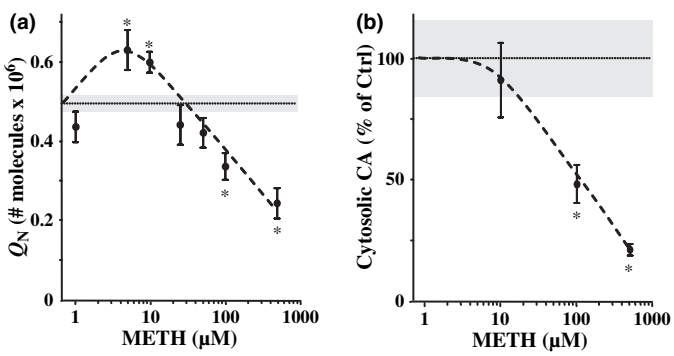

Fig. 6 METH concentration dependences of vesicular and cytosolic catecholamine contents. (a) Quantal size versus METH concentration in cells treated with the drug for 24 h. Data are presented as the mean ± SEM of the median Q_N values from individual cells (n = 97 cells in control and 11–43 in METH-treated groups). (b) Cytosolic catecholamine concentrations in cells incubated with METH for 24 h (n = 22–46 cells); $^*p < 0.05$ compared with untreated cells. Dotted line and shadowed box represent the mean ± SEM in untreated cells.

between the concentration of METH and quantal size in cells treated with METH for 24 h was bell-shaped. At low-micromolar METH concentrations (5–10 μM) the amount of catecholamine released per vesicle was significantly increased, while at higher concentrations (100–500 μM) that are often employed in studies of METH-induced neurotoxicity *in vitro*, quantal size was decreased by as much as 50% (Fig. 6a).

Vesicular catecholamine is generally thought to be at equilibrium with cytosolic transmitter concentration (Leviel *et al.* 1989; Chien *et al.* 1990). To investigate the discrepancy between unexpectedly low quantal sizes observed in hyperacidified vesicles following prolonged exposure to METH, we checked whether cytosolic catecholamines were affected by long exposures to the highest drug levels (100–500 μM) that are known to up-regulate macroautophagy, a pathway that can lead to a bulk degradation of cytosolic content (Larsen *et al.* 2002). Using intracellular patch electrochemistry (IPE), we have previously shown that even though free cytosolic transmitter concentration increases several-fold in chromaffin cells acutely treated with 50 μM AMPH, it returns to initial levels after ~30 min of exposure (Mosharov *et al.* 2003). IPE measurements in cells treated with high-micromolar METH concentrations for 24 h showed that cytosolic catecholamines were indeed significantly lower than those found in untreated cells (Fig. 6b), which may underlie the reduction in quantal size at high, possibly cytotoxic METH concentrations (Fig. 6a). Macroautophagy, which can be induced by prolonged METH treatment (Larsen *et al.* 2002; Talloczy *et al.* 2008) did not play a significant role in the regulation of quantal size, as seen by a lack of effect by macroautophagy blockade (Fig. S2).

Next, we investigated the changes in amperometric quantal events induced by pharmacologically relevant low-micromolar METH doses (see Materials and methods) in further detail. In agreement with previous reports (Sulzer *et al.* 1992;

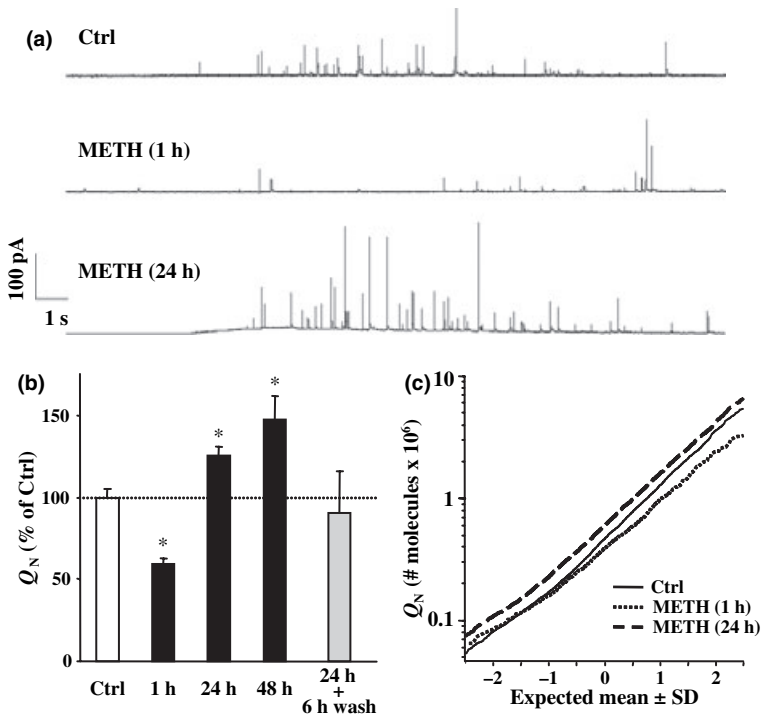

Fig. 7 Effects of 10 μM METH on exocytotic quantal size in chromaffin cells. (a) Representative amperometric recordings of quantal catecholamine release from untreated cells and cells exposed to 10 μM METH for 1 h or 24 h. (b) Time dependence of quantal sizes in cells incubated with 10 μM METH. After 24 h of treatment, the cells were washed with drug-free media and incubated for additional 6 h before the amperometric recordings (gray bar). Data presented as percentages of changes relative to matched untreated sister cultures at the same day; $^*p < 0.05$ compared with untreated cells (see also Table 1). (c) Normal probability plots of the Log-transformed Q_N from untreated cells ($n = 6522$ events) and cells treated with 10 μM METH for 1 h ($n = 963$ events), or 24 h ($n = 3045$).

Table 1 Comparative characteristics of amperometric events recorded from chromaffin cells treated with 10 μM METH

	Inter-spike interval	Events/stimulation	$t_{½}$	I_{max}	Q_N	t_{rise} (25–75%)	Rise slope	Fall τ_1	Fall τ_2
1 h METH	112 ± 17	106 ± 11	136 ± 9*,[a]	38 ± 3*	59 ± 4*	168 ± 15*	26 ± 5*	216 ± 16*	164 ± 26*
24 h METH	111 ± 16	111 ± 7	102 ± 8	143 ± 9*	126 ± 5*	98 ± 5	203 ± 26*	95 ± 9	102 ± 6
48 h METH	91 ± 13	90 ± 3	94 ± 14	148 ± 29*	146 ± 17*	102 ± 9	173 ± 69*	82 ± 14	114 ± 19

The median values of each parameter were first calculated for amperometric events recorded from individual cells and then the average of the medians was computed. The data are presented as percentages of changes in amperometric spike characteristics relative to matched controls recorded from sister cultures at the same day ($n = 85$ cells for control, 30 cells for 1 h METH, 72 cells for 24 h METH, and 15 cells for 48 h METH). For absolute values of spike parameters in control cells and those treated with 10 μM METH for 24 h see Table S1.

[a]Although $t_{½}$ was significantly increased in cells acutely treated with METH, this might be resulting from several reasons, including alteration of the fusion pore kinetics or the composition of the intravesicular matrix. It is also possible that smaller amperometric spikes are more affected by the noise and thereby have longer $t_{½}$ resulting from artifact (Mosharov and Sulzer 2005).

$^*p < 0.05$ versus untreated cells.

Sulzer *et al.* 1995; Mundorf *et al.* 1999), acute 1 h exposure to 10 μM METH decreased the amplitudes of amperometric events (I_{max}) and the number of catecholamine molecules exocytosed from individual vesicle fusion events (Q_N) (Fig. 7a and b and Table 1). Analysis of quantal size distributions using a normal probability plot (Sulzer and Pothos 2000) revealed that acute exposure to METH produced a downward shift of the population of quantal sizes (Fig. 7c).

In marked contrast to the acute effects of METH, 24 or 48 h exposure to 10 μM METH increased quantal size by 26% and 48%, respectively, also enlarging the average I_{max} of amperometric events (Fig. 7b, Table 1). No significant difference was detected between cytosolic catecholamine levels in untreated cells and cells incubated with 10 μM METH (Fig. 6b). Quantal sizes from cells treated for 1 or 2 days displayed a uniform upward shift on the normal probability plot, indicating that transmitter release was increased by the same percentage in all secretory vesicles, regardless of their pre-treatment catecholamine content (Fig. 7c). These data demonstrate that at low, pharmacologically relevant METH concentrations and exposure times, vesicular quantal size can be augmented by AMPHs, in contrast to the predictions from the weak base model of

AMPH action but consistent with the effect of secretory vesicle rebound hyperacidification.

Discussion

Neurosecretory vesicles can modulate their transmitter content and quantal size even after maturation (Sulzer and Pothos 2000; Edwards 2007). One of the regulatory mechanisms that can alter the amount of stored vesicular catecholamine is an adjustment of intravesicular pH gradient created by the vH^+-ATPase (Johnson 1988). Studies on isolated chromaffin vesicles have established that they reach a stable pH of ~5.5 (Winkler and Westhead 1980), which provides a driving force for the transport of catecholamines into vesicles against an adverse $\sim 10^5$ concentration gradient of transmitter between the vesicle interior and the cytosol (Johnson 1988). When the acidic intravesicular pH is collapsed by the vH^+-ATPase inhibitor bafilomycin A (Zhou *et al.* 2000; Pothos *et al.* 2002) or following acute exposure to weak bases such as chloroquine, ammonia, or AMPHs (Van der Kloot 1987; Sulzer *et al.* 1995; Mundorf *et al.* 1999; Camacho *et al.* 2006), there is a decrease in the number of catecholamine molecules released per exocytotic event. Using a combination of optical and electrochemical techniques, we confirm that acute METH exposure alkalinized chromaffin vesicles and decreases exocytotic quantal size, but further identified a previously unsuspected rebound vesicle hyperacidification that eventually overcompensated for the initial collapse of the transmembrane proton gradient.

The ability of secretory vesicles to undergo rebound hyperacidification was shown by live optical measurements of intravesicular acidity with AO and LSYB and by the quantitative immunoelectron microscopic measurement of DAMP. Under the same conditions of exposure to METH, the effect of rebound hyperacidification estimated in living cells by ratiometric measurements with LSYB (ΔpH 1.2) was larger than that estimated ultrastructurally with DAMP (ΔpH 0.6). Both approaches, however, are based on the partition of lipophilic weak bases according to the intracellular pH gradients and are susceptible to experimental artifacts that can result in different apparent pH values. Intravesicular pH estimated from the partitioning of DAMP would be increased if DAMP were to diffuse out of vesicles during fixation. A slight efflux of DAMP out of vesicles might be expected to occur unless its coupling to protein by fixation was so rapid as to be almost instantaneous; the immunocytochemical detection of DAMP accumulation, therefore, probably underestimates the degree of intravesicular acidity. Indeed, our current DAMP-derived estimates in untreated cells (pH 5.7) were slightly more basic than those determined by alternative methods (pH 5.5) (Pollard *et al.* 1979; Njus *et al.* 1986; Johnson 1988) or by LSYB (pH 5.4). On the other hand, while LSYB does not require fixation, it is possible that LSYB spectrum may change when the dye accumulates to a high concentration inside of vesicles, as occurs with AO (Mason and McCaffery 1964; Lee and Forte 1980), or that other factors affect its accumulation or calibration. If the LSYB measurements are accurate, the intravesicular acidity below pH 4.0 in cells treated with 100–500 μM METH (Fig. 2e) would be unexpectedly low for mammalian vesicles, although secretory organelles in plants and some algae equipped with essentially the same vH^+-ATPase maintain a pH below 2.0 (Ziegler *et al.* 1995; Muller *et al.* 1996). While it is not clear which approach more accurately reflects intravesicular pH, both methods were consistent in demonstrating rebound hyperacidification of secretory vesicles.

Both the initial pH collapse and the rebound hyperacidification depended similarly on the METH concentration, suggesting that one might be a delayed consequence of the other. The process was reversible, independent of *de novo* protein synthesis, and occurred at a higher rate upon re-exposure to METH. Rebound hyperacidification, moreover, occurred with a variety of weak bases, and may result from the cytosolic acidification and decreased vesicular/cytosolic pH concentration gradient well known to follow weak base withdrawal, the latter of which is activated by a Ca^{2+}-dependent compensatory increase in proton uptake (Burns *et al.* 1991). This mechanism is consistent with recent findings showing that intravesicular Ca^{2+} is displaced into the cytosol in cells acutely exposed to weak bases (Mundorf *et al.* 1999), that Ca^{2+} entry causes transient acidification of chromaffin vesicles (Camacho *et al.* 2006), and that stimulation-dependent chromaffin vesicle acidification is dependent on Ca^{2+} entry (Pothos *et al.* 2002). We cannot, however, rule out the participation of additional mechanisms, including delivery and assembly of V_0 and V_1 subunits of the vH^+-ATPase, a process described for human and porcine epithelial cells and yeast cells (Kane and Smardon 2003; Sautin *et al.* 2005; Beyenbach and Wieczorek 2006), a compensation of the ion gradients across the vesicle membrane (Grabe and Oster 2001; Demaurex 2002; Li *et al.* 2002), or an alteration in the permeability of vesicular membranes to protons, the so-called 'proton leak' (Diwu *et al.* 1999; Grabe and Oster 2001; Demaurex 2002).

An important functional consequence of METH-induced vesicle rebound hyperacidification is the corresponding alteration of quantal size of stimulation-dependent exocytosis. At low METH doses, when cytosolic catecholamine concentration was apparently unaffected, there was a nearly linear relationship between quantal size and the square of the intravesicular proton concentration (Fig. 8), in agreement with predictions from studies on isolated chromaffin vesicles (Johnson 1988; Maycox *et al.* 1990) (see Materials and methods). Increased quantal size after prolonged METH treatment was uniform for all vesicles, as indicated by an upward shift of the entire quantal size distribution when displayed as a normal probability plot.

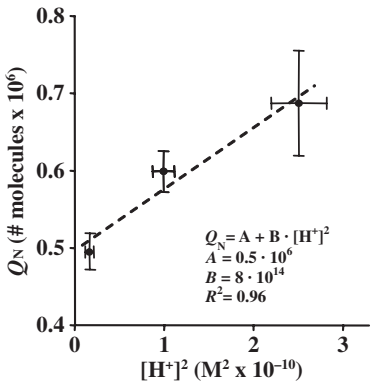

Fig. 8 Relationship between the square of the vesicle proton concentration and quantal size. The values for Q_N are the averages of cell medians from untreated cells and those treated with 10 μM METH for 24 and 48 h. The square of the vesicular proton concentration, which has been found in empirical studies to be directly related to vesicular catecholamine concentration (see Materials and methods), was calculated from ratiometric pH measurements as: $[H^+]^2 = (10^{-pH})^2$.

The effects of METH on quantal size, however, were different at the highest drug concentrations. Although there was a substantial rebound hyperacidification at these levels, the quantal size was decreased. Possible reasons for the bell-shaped dependence of quantal size on the METH concentration include the effects of METH on catecholamine vesicular uptake transporter (Brown *et al.* 2000; Partilla *et al.* 2006), and the ability of high METH concentrations to induce neurotoxicity associated with an autophagic stress response (Larsen *et al.* 2002). The latter possibility is supported by the decrease in cytosolic catecholamine observed exclusively at higher drug levels that are employed in METH neurotoxicity studies (Bennett *et al.* 1993; Stumm *et al.* 1999; Larsen *et al.* 2002; Jimenez *et al.* 2004). Therefore, at high METH doses vesicular catecholamine uptake appears to be limited not by the acidity of the vesicles, but by the availability of the cytosolic catecholamine.

Overall, we found that at METH concentrations (5–10 μM) and incubation times (24–48 h) that may be close to those found in drug abusers and ADHD patients (see Materials and methods), the net output of all processes affecting intracellular catecholamine homeostasis was to increase stimulation-dependent catecholamine release. Thus, while acute METH reduces the signal from evoked, stimulation-dependent release, prolonged METH renormalizes and could even enhance the stimulation-dependent exocytotic catecholamine release. As evoked catecholamine release is thought to reflect the incentive value of external stimuli to attention and working memory (Waelti *et al.* 2001) and as AMPHs are used to treat fatigue and attention deficit disorders, an ability of prolonged low levels of AMPHs administration to increase quantal size could contribute to their therapeutic effects.

Acknowledgements

We thank Drs Mark Sonders and François Gonon for helpful discussions. This study was funded by the Picower Foundation, NIDA, and the Parkinson's Disease Foundation.

Supporting information

Additional Supporting Information may be found in the online version of this article:

Fig. S1 Protocol for LysoSensor Yellow/Blue *in situ* calibration.

Fig. S2 Changes in amperometric quantal size in cells exposed to 500 μM METH for 24 h in the absence and in the presence of autophagy inhibitor 3-MA (10 mM).

Table S1 Absolute values for the characteristics of amperometric events recorded from chromaffin cells treated with 10 μM METH for 24 h.

Please note: Wiley-Blackwell are not responsible for the content or functionality of any supporting materials supplied by the authors. Any queries (other than missing material) should be directed to the corresponding author for the article.

References

Anderson R. G., Falck J. R., Goldstein J. L. and Brown M. S. (1984) Visualization of acidic organelles in intact cells by electron microscopy. *Proc. Natl Acad. Sci. USA* **81**, 4838–4842.

Bennett B. A., Hyde C. E., Pecora J. R. and Clodfelter J. E. (1993) Differing neurotoxic potencies of methamphetamine, mazindol, and cocaine in mesencephalic cultures. *J. Neurochem.* **60**, 1444–1452.

Beyenbach K. W. and Wieczorek H. (2006) The V-type H+ ATPase: molecular structure and function, physiological roles and regulation. *J. Exp. Biol.* **209**, 577–589.

Brown J. M., Hanson G. R. and Fleckenstein A. E. (2000) Methamphetamine rapidly decreases vesicular dopamine uptake. *J. Neurochem.* **74**, 2221–2223.

Bruns D. and Jahn R. (1995) Real-time measurement of transmitter release from single synaptic vesicles. *Nature* **377**, 62–65.

Burdon R. H., Kerr S. M., Cutmore C. M., Munro J. and Gill V. (1984) Hyperthermia, Na^+ K^+ ATPase and lactic acid production in some human tumour cells. *Br. J. Cancer* **49**, 437–445.

Burns K. D., Homma T., Breyer M. D. and Harris R. C. (1991) Cytosolic acidification stimulates a calcium influx that activates Na(+)-H^+ exchange in LLC-PK1. *Am. J. Physiol.* **261**, F617–F625.

Camacho M., Machado J. D., Montesinos M. S., Criado M. and Borges R. (2006) Intragranular pH rapidly modulates exocytosis in adrenal chromaffin cells. *J. Neurochem.*. **96**, 324–334 [Epub 2005 Dec 2008].

Chien J. B., Wallingford R. A. and Ewing A. G. (1990) Estimation of free dopamine in the cytoplasm of the giant dopamine cell of Planorbis corneus by voltammetry and capillary electrophoresis. *J. Neurochem.* **54**, 633–638.

Cho A. K., Melega W. P., Kuczenski R. and Segal D. S. (2001) Relevance of pharmacokinetic parameters in animal models of methamphetamine abuse. *Synapse* **39**, 161–166.

Cook C. E., Jeffcoat A. R., Sadler B. M., Hill J. M., Voyksner R. D., Pugh D. E., White W. R. and Perez-Reyes M. (1992) Pharmacokinetics of oral methamphetamine and effects of repeated daily dosing in humans. *Drug Metab. Dispos.* **20**, 856–862.

Cravey R. H. and Baselt R. C. (1968) Methamphetamine poisoning. *J. Forensic. Sci. Soc.* **8**, 118–120.

Demaurex N. (2002) pH Homeostasis of cellular organelles. *News Physiol. Sci.* **17**, 1–5.

Diwu Z., Chen C. S., Zhang C., Klaubert D. H. and Haugland R. P. (1999) A novel acidotropic pH indicator and its potential application in labeling acidic organelles of live cells. *Chem. Biol.* **6**, 411–418.

Edwards R. H. (2007) The neurotransmitter cycle and quantal size. *Neuron.* **55**, 835–858.

Finnegan J. M., Pihel K., Cahill P. S., Huang L., Zerby S. E., Ewing A. G., Kennedy R. T. and Wightman R. M. (1996) Vesicular quantal size measured by amperometry at chromaffin, mast, pheochromocytoma, and pancreatic beta-cells. *J. Neurochem.* **66**, 1914–1923.

Fischer J. F. and Cho A. K. (1979) Chemical release of dopamine from striatal homogenates: evidence for an exchange diffusion model. *J. Pharmacol. Exp. Therapeu.* **208**, 203–209.

Gettig J. P., Grady S. E. and Nowosadzka I. (2006) Methamphetamine: putting the brakes on speed. *J. Sch. Nurs.* **22**, 66–73.

Grabe M. and Oster G. (2001) Regulation of organelle acidity. *J. Gen. Physiol.* **117**, 329–344.

Harris D. S., Boxenbaum H., Everhart E. T., Sequeira G., Mendelson J. E. and Jones R. T. (2003) The bioavailability of intranasal and smoked methamphetamine. *Clin. Pharmacol. Ther.* **74**, 475–486.

Holopainen J. M., Saarikoski J., Kinnunen P. K. and Jarvela I. (2001) Elevated lysosomal pH in neuronal ceroid lipofuscinoses (NCLs). *Eur. J. Biochem.* **268**, 5851–5856.

Jimenez A., Jorda E. G., Verdaguer E., Pubill D., Sureda F. X., Canudas A. M., Escubedo E., Camarasa J., Camins A. and Pallas M. (2004) Neurotoxicity of amphetamine derivatives is mediated by caspase pathway activation in rat cerebellar granule cells. *Toxicol. Appl. Pharmacol.* **196**, 223–234.

Johnson R. G. (1988) Accumulation of biological amines into chromaffin granules: a model for hormone and neurotransmitter transport. *Physiol. Rev.* **68**, 232–307.

Jones A. W. and Holmgren A. (2005) Abnormally high concentrations of amphetamine in blood of impaired drivers. *J. Forensic. Sci.* **50**, 1215–1220.

Jones S. R., Gainetdinov R. R., Wightman R. M. and Caron M. G. (1998) Mechanisms of amphetamine action revealed in mice lacking the dopamine transporter. *J. Neurosci.* **18**, 1979–1986.

Kahlig K. M., Binda F., Khoshbouei H., Blakely R. D., McMahon D. G., Javitch J. A. and Galli A. (2005) Amphetamine induces dopamine efflux through a dopamine transporter channel. *Proc. Natl. Acad. Sci. USA* **102**, 3495–3500.

Kane P. M. and Smardon A. M. (2003) Assembly and regulation of the yeast vacuolar H+-ATPase. *J. Bioenerg. Biomembr.* **35**, 313–321.

Keech M. L. and Wills E. D. (1979) The effect of hyperthermia on activation of lysosomal enzymes in HeLa cells. *Eur. J. Cancer* **15**, 1025–1031.

Kim I., Oyler J. M., Moolchan E. T., Cone E. J. and Huestis M. A. (2004) Urinary pharmacokinetics of methamphetamine and its metabolite, amphetamine following controlled oral administration to humans. *Ther. Drug. Monit.* **26**, 664–672.

Larsen K. E., Fon E. A., Hastings T. G., Edwards R. H. and Sulzer D. (2002) Methamphetamine-induced degeneration of dopaminergic neurons involves autophagy and upregulation of dopamine synthesis. *J. Neurosci.* **22**, 8951–8960.

Lee H. C. and Forte J. G. (1980) A novel method for measurement of intravesicular pH using fluorescent probes. *Biochim. Biophys. Acta* **601**, 152–166.

Leviel V., Gobert A. and Guibert B. (1989) Direct observation of dopamine compartmentation in striatal nerve terminal by 'in vivo' measurement of the specific activity of released dopamine. *Brain Res.* **499**, 205–213.

Li X., Wang T., Zhao Z. and Weinman S. A. (2002) The ClC-3 chloride channel promotes acidification of lysosomes in CHO-K1 and Huh-7 cells. *Am. J. Physiol. Cell Physiol.* **282**, C1483–C1491.

Mason S. F. and McCaffery A. J. (1964) Optical rotatory power of DNA and of its complex with acridine orange under streaming conditions. *Nature* **204**, 468–470.

Maycox P. R., Hell J. W. and Jahn R. (1990) Amino acid neurotransmission: spotlight on synaptic vesicles. *Trends Neurosci.* **13**, 83–87.

Melega W. P., Williams A. E., Schmitz D. A., DiStefano E. W. and Cho A. K. (1995) Pharmacokinetic and pharmacodynamic analysis of the actions of D-amphetamine and D-methamphetamine on the dopamine terminal. *J. Pharmacol. Exp. Ther.* **274**, 90–96.

Mosharov E. V. and Sulzer D. (2005) Analysis of exocytotic events recorded by amperometry. *Nat. Methods* **2**, 651–658.

Mosharov E., Gong L.-W., Khanna B., Lindau M. and Sulzer D. (2003) Intracellular patch electrochemistry: regulation of cytosolic catecholamines in chromaffin cells. *J. Neurosci.* **23**, 5835–5845.

Muller M., Irkens-Kiesecker U., Rubinstein B. and Taiz L. (1996) On the mechanism of hyperacidification in lemon. Comparison of the vacuolar H(+)-ATPase activities of fruits and epicotyls. *J. Biol. Chem.* **271**, 1916–1924.

Mundorf M. L., Hochstetler S. E. and Wightman R. M. (1999) Amine weak bases disrupt vesicular storage and promote exocytosis in chromaffin cells. *J. Neurochem.* **73**, 2397–2405.

Njus D., Kelley P. M. and Harnadek G. J. (1986) Bioenergetics of secretory vesicles. *Biochim. Biophys. Acta* **853**, 237–265.

Orci L., Halban P., Perrelet A., Amherdt M., Ravazzola M. and Anderson R. G. (1994) pH-independent and -dependent cleavage of proinsulin in the same secretory vesicle. *J. Cell Biol.* **126**, 1149–1156.

Orrenius S. and Maehly A. C. (1970) Lethal amphetamine intoxication. A report of three cases. *Z. Rechtsmed.* **67**, 184–189.

Partilla J. S., Dempsey A. G., Nagpal A. S., Blough B. E., Baumann M. H. and Rothman R. B. (2006) Interaction of amphetamines and related compounds at the vesicular monoamine transporter. *J. Pharmacol. Exp. Ther.* **319**, 237–246 [Epub 2006 Jul 2011].

Perez-Reyes M., White W. R., McDonald S. A., Hicks R. E., Jeffcoat A. R., Hill J. M. and Cook C. E. (1991) Clinical effects of daily methamphetamine administration. *Clin. Neuropharmacol.* **14**, 352–358.

Pollard H. B., Shindo H., Creutz C. E., Pazoles C. J. and Cohen J. S. (1979) Internal pH and state of ATP in adrenergic chromaffin granules determined by 31P nuclear magnetic resonance spectroscopy. *J. Biol. Chem.* **254**, 1170–1177.

Pothos E. N., Mosharov E., Liu K. P., Setlik W., Haburcak M., Baldini G., Gershon M. D., Tamir H. and Sulzer D. (2002) Stimulation-dependent regulation of the pH, volume and quantal size of bovine and rodent secretory vesicles. *J. Physiol.* **542**, 453–476.

Riviere G. J., Gentry W. B. and Owens S. M. (2000) Disposition of methamphetamine and its metabolite amphetamine in brain and other tissues in rats after intravenous administration. *J. Pharmacol. Exp. Ther.* **292**, 1042–1047.

Sautin Y. Y., Lu M., Gaugler A., Zhang L. and Gluck S. L. (2005) Phosphatidylinositol 3-kinasemediated effects of glucose on vacuolar H+-ATPase assembly, translocation, and acidification of intracellular compartments in renal epithelial cells. *Mol. Cell. Biol.* **25**, 575–589.

Schepers R. J., Oyler J. M., Joseph R. E. Jr., Cone E. J., Moolchan E. T. and Huestis M. A. (2003) Methamphetamine and amphetamine pharmacokinetics in oral fluid and plasma after controlled oral methamphetamine administration to human volunteers. *Clin. Chem.* **49**, 121–132.

Sonders M. S., Zhu S. J., Zahniser N. R., Kavanaugh M. P. and Amara S. G. (1997) Multiple ionic conductances of the human dopamine transporter: the actions of dopamine and psychostimulants. *J. Neurosci.* **17**, 960–974.

Steyer J. A., Horstmann H. and Almers W. (1997) Transport, docking and exocytosis of single secretory granules in live chromaffin cells. *Nature* **388**, 474–478.

Stumm G., Schlegel J., Schafer T., Wurz C., Mennel H. D., Krieg J. C. and Vedder H. (1999) Amphetamines induce apoptosis and regulation of bcl-x splice variants in neocortical neurons. *Faseb J.* **13**, 1065–1072.

Sulzer D. and Pothos E. N. (2000) Regulation of quantal size by presynaptic mechanisms. *Rev. Neurosci.* **11**, 159–212.

Sulzer D. and Rayport S. (1990) Amphetamine and other psychostimulants reduce pH gradients in midbrain dopaminergic neurons and chromaffin granules: a mechanism of action. *Neuron* **5**, 797–808.

Sulzer D., Pothos E., Sung H. M., Maidment N. T., Hoebel B. G. and Rayport S. (1992) Weak base model of amphetamine action. *Ann. NY Acad. Sci.* **654**, 525–528.

Sulzer D., Chen T., Lau Y., Kristensen H., Rayport S. and Ewing A. (1995) Amphetamine redistributes dopamine from synaptic vesicles to the cytosol and promotes reverse transport. *J. Neurosci.* **15**, 4102–4108.

Sulzer D., Sonders M. S., Poulsen N. W. and Galli A. (2005) Mechanisms of neurotransmitter release by amphetamines: a review. *Prog. Neurobiol.* **75**, 406–433.

Tabb J. S., Kish P. E., Van Dyke R. and Ueda T. (1992) Glutamate transport into synaptic vesicles. Roles of membrane potential, pH gradient, and intravesicular pH. *J. Biol. Chem.* **267**, 15412–15418.

Talloczy Z., Martinez J., Joset D. *et al.* (2008) Methamphetamine inhibits antigen processing, presentation, and phagocytosis. *PLoS Pathog.* **4**, e28.

Van der Kloot W. (1987) Inhibition of packing of acetylcholine into quanta by ammonium. *Faseb J.* **1**, 298–302.

Waelti P., Dickinson A. and Schultz W. (2001) Dopamine responses comply with basic assumptions of formal learning theory. *Nature* **412**, 43–48.

Winkler H. and Westhead E. (1980) The molecular organization of adrenal chromaffin granules. *Neuroscience* **5**, 1803–1823.

Zhou Q., Petersen C. C. and Nicoll R. A. (2000) Effects of reduced vesicular filling on synaptic transmission in rat hippocampal neurones. *J. Physiol.* **525**, 195–206.

Ziegler K., Hauska G. and Nelson N. (1995) Cyanidium caldarium genes encoding subunits A and B of V-ATPase. *Biochim. Biophys. Acta.* **1230**, 202–206.